5 Understanding The Hubbard Model With Simple Calculations

Richard T. Scalettar
University of California Davis
Department of Physics and Astronomy, One Shields Ave., Davis, CA 95616

Contents

1 Introduction **2**

2 A classical mechanics prelude **3**

3 Mean Field Theory **11**

4 Particle-Hole Symmetry **11**

5 Staggered Particle-Particle Transformation **11**

A Some remarks **12**

1 Introduction

A discussion of the Hubbard Hamiltonian is a truly immense undertaking. From a temporal point of view it encompasses a six decade history spanning the work of Hubbard, Anderson and Mott in the 1960's through a host of materials to which it has been applied: transition metal oxides, heavy fermions, cuprate superconductors, etc [1]. Indeed, in the last 15 years a major focus of the Atomic and Molecular (AMO) community has been on realizing and characterizing the Hubbard model in systems of ultracold atoms [2, 3]. Attempts to solve the Hubbard model computationally have driven a rich set of stories in inhomogeneous Hartree-Fock (stripe formation) [4], Quantum Monte Carlo (QMC) [5] (including the famous 'sign problem'), density matrix renormalization group (DMRG) methods [6], and machine learning [7]. A recent review summarizes the breadth of these developments, applications and connections [8].

From a pedagogical point of view, the danger of a lecture (or even several lectures) on the Hubbard model is the temptation to do too much. The audience is then left with a sense of the breadth and excitement of the field, but not with a concrete ability to '*do something*'.

The objectives of this lecture are to provide some specific calculations which shed light on the basic physics of the Hubbard model. We will begin with the non-interacting limit, i.e. obtaining the 'band structure' of the Hubbard model. We will emphasize that this already allows contact with some fascinating phenomena- localization by disorder, Fermi surface nesting and a divergence of the density of states linked to magnetism and superconductivity, and flat bands in which the electron energy is independent of momentum.

We will also take a couple of detours into some relatively new and fascinating aspects of the non-interacting Hubbard model: a prescription for the achievement of 'perfect quantum state transfer' and the effect of 'non-Hermiticity' where the motion of fermions to the left and to the right is unbalanced (the 'Hatano-Nelson' model).

Although this first discussion leaves interactions out entirely, it establishes the computational foundation for their inclusion at the mean-field level. This will be our second topic. We will not attempt any more sophisticated treatment of correlations here (diagrammatic Greens function methods, QMC, DMRG, $\cdots$.)

The final objective is to describe the consequences of a set of canonical transformations which can be performed on the Hubbard model. We will see these allow us to discern surprising and not immediately intuitive physics in some parameter regimes from the more evident physics in others. Our first illustration will be on the by now well-known connections between magnetism in the repulsive Hubbard models and s-wave superconductivy and charge density wave formation in the attractive Hubbard model. We will then turn to a recent discovery of a tranformation which leads to a rigorous demonstration of a model exhibiting pair density wave formation, a phase of matter which has proven elusing to achieve both experimentally and theoretically.

2 A classical mechanics prelude

Let's begin with a familiar, but seemingly completely unrelated problem, which will prove to have close mathematical analogies with the non-interacting Hubbard model. Consider a one-dimensional array of N uniform masses m connected to their neighbors by uniform springs γ. Newton's equations of motion are,

$$m\frac{d^2x_l}{dt^2} = -\gamma\big(\,x_l - x_{l+1}\,\big) - \gamma\big(\,x_l - x_{l-1}\,\big) \tag{1}$$

where $x_l(t)$ is the displacement from equilibrium of mass l at time t. We solve this problem with the *ansatz* $x_l(t) = a_l\, e^{i\omega t}$ which reduces the N coupled differential equations to N coupled algebraic equations for the amplitudes a_l. After cancelling the common factor of $a_0\, e^{i\omega t}$ from all the terms,

$$m\omega^2\, a_l = \gamma\big(\,a_l - a_{l+1}\,\big) + \gamma\big(\,a_l - a_{l-1}\,\big) \tag{2}$$

These equations are solved by introducing normal mode coordinates

$$a_l = e^{-ikl}a_0, \tag{3}$$

yielding the normal mode frequencies

$$\omega^2(k) = 2\gamma\big(1 - \cos(k)\big) \tag{4}$$

where we have now used notation emphasizing the frequency depends on the 'momentum' k. (We will come back shortly to why calling k the momentum makes sense.)

Eq. 4 is an embarassment of riches. From a collection of N linear equations (Eqs. 2) we have an *infinite* set of solutions labeled by the continuous parameter k. Something is wrong, and it's because we did not treat the boundary conditions carefully. Equations 2 are only true for the masses which have both left and right neighbors, $l = 2, 3, \cdots N$-1. The two masses at the end have only a single neighbor if we adopt 'open boundary conditions' (obc). Here instead we use 'periodic boundary conditions' (pbc), and link oscillator $l = 1$ to oscillator $l = N$ with an extra spring of potential energy $\frac{1}{2}\gamma(x_1 - x_N)^2$. Then Eqs. 2 apply to *all* x_l, if we demand that $x_0 \equiv x_N$ and $x_1 \equiv x_{N+1}$.

This solves our problem of too many solutions, since it quantizes the previously unrestricted allowed values of momentum by requiring $e^{ikN} = 1$ or, in other words, $k \in \frac{2\pi}{N}\{1, 2, \cdots, N\}$. Because cosine is periodic, it is equivalent to set $k = \frac{2\pi}{N}\{-\frac{N}{2} + 1, -\frac{N}{2} + 2 \cdots \frac{N}{2}\}$. which has the advantage of making k more symmetric about $k = 0$.

It is useful to consider two special cases. When $k = 0$ all masses have identical displacements $a_l = a_0$. The entire chain is shifted rigidly and $\omega(k) = 0$. This is an example of a zero frequency 'Goldstone mode' associated with the translational invariance of our mass-spring system. (Because only inter-mass springs are present, there is no potential tying any mass

to a particular location in space. As a sequence the energy is invariant under a simultaneous translation of all the masses. Put another way, the choice of origin is irrelevant.) On the other hand, when $k = \pi$ the masses alternate $a_l = a_0\, e^{i\pi l} = a_0(-1)^l$. This results in the largest normal mode frequency (energy), $\omega^2 = \frac{4k}{m}$. (There is an interesting analogy with quantum mechanics here. If you sketch a_l versus l for this highest energy mode, you see there is a node between every mass. a_l wiggles as fast as possible. Similarly, in quantum mechanics we know that wiggly wave functions are associated with high kinetic energy.)

One can also solve the obc case. The 'dispersion relation' giving the functional form for $\omega(k)$ is unchanged, but the N allowed momenta are shifted slightly to $k \in \frac{2\pi}{N+1}\{0, 1, 2, \cdots N\text{-}1\}$. The pbc case is a bit more simple, so we use it here. Besides simplicity, it is also the case that properties measured in finite length N chains with pbc are closer to the thermodynamic limit $N = \infty$ than obc. (Specifically, finite size corrections often go as $\frac{1}{N^2}$ with pbc and $\frac{1}{N}$ with obc.)

A closing observation is that this solution of coupled oscillators all goes horribly wrong in the presence of anharmonicity. Indeed, even a single anharmonic oscillator, the solution of $F = ma$ with $V(x) = \frac{1}{2}kx^2 + \frac{1}{4}ux^4$ is intractable. As we shall see below, the presence of quartic terms ux^4 in the fermion creation and destruction operators are precisely what makes the Hubbard model impossible to solve for U non-zero.

That's a long time spent on classical mechanics! But we will see now that the exact same mathematics underlies the solution of the non-interacting Hubbard model.
Let's write down the non-interacting Hubbard model for a 1D chain.

$$\hat{\mathcal{H}} = -t \sum_l \left(\hat{c}^\dagger_{l\sigma} \hat{c}_{l+1\,\sigma} + \hat{c}^\dagger_{l+1\,\sigma} \hat{c}_{l\sigma} \right) - \mu \sum_l \hat{c}^\dagger_{l\sigma} \hat{c}_{l\sigma} \tag{5}$$

I am going to assume we are all familiar with the basic properties of fermion creation and destruction operators $\hat{c}^\dagger_{l\sigma}$ and $\hat{c}_{l\sigma}$, including, for example, their anticommutation relations, $\left\{\hat{c}^\dagger_{l\sigma}, \hat{c}_{j\sigma}\right\} = \delta_{jl}\delta_{\sigma\sigma'}$ and $\left\{\hat{c}^\dagger_{l\sigma}, \hat{c}^\dagger_{j\sigma}\right\} = 0$. The first two terms in Eq. 5 describe the hopping of a fermion from right-to-left and from left-to-right respectively. The third term is the 'chemical potential'. It alows us to control the number of fermions. Because we will not have any interactions for this part of the discussion, we will suppress the spin index σ on the fermionic operators. That is, since U is the only thing that connects fermions with $\sigma =\uparrow$ to fermions with $\sigma =\downarrow$, when $U = 0$ we can just solve each spin sector independently.

Now just as we defined normal mode coordinates for the positions of our masses we can also here define linear combinations of

$$\hat{c}^\dagger_k \equiv \frac{1}{\sqrt{N}} \sum_l e^{ikl} \hat{c}^\dagger_l \tag{6}$$

and its inverse,

$$\hat{c}^\dagger_l \equiv \frac{1}{\sqrt{N}} \sum_l e^{-ikl} \hat{c}^\dagger_k. \tag{7}$$

Note the reemblance between Eqs. 6 and 3. The fermion creation operator transformation is, however, a little more subtle than the classical mechanics case, because we must be sure that our new operators $\hat{c}_k$ obey the same fermionic anti-commutation relations as the originals. It is easy to prove this from the identities

$$\frac{1}{N}\sum_l e^{i(k-k')l} = \delta_{kk'} \tag{8}$$

and

$$\frac{1}{N}\sum_k e^{i(l-l')k} = \delta_{ll'} \tag{9}$$

which hold for the discrete allowed momenta $k, k' \in \frac{2\pi}{N}\{-\frac{N}{2}+1, -\frac{N}{2}+2 \cdots \frac{N}{2}\}$. Equations and are the discrete analogs of the familiar orthogonality relations used in Fourier transforms.

Plugging the transformation Eq. 7 into the Hamiltonian, Eq. 5, and making use of Eqs. 2 and 2 yields

$$\hat{\mathcal{H}} = \sum_k \big(E_k - \mu \big) \hat{c}_k^\dagger \hat{c}_k \tag{10}$$

where

$$E(k) = -2t\cos(k) \tag{11}$$

The similarity between the right-hand sides of Eqs. 4 and 11 should be evident, from the appearance of $\cos(k)$ to $2\gamma \leftrightarrow -\mu$. The energy levels of the 1D Hubbard chain range from $-2t \leq E(k) \leq +2t$. One refers to this range as the 'bandwidth' $W = 4t$.

It is interesting to think about the physics of the structure on Eq. 10. The Hamiltonian does not 'mix' different values of momentum k. When an electron of momentum k is destroyed, all that can happen is that an electron with the *same* momentum be created. This is the analog of the classical mechanical principal that normal modes do not mix: A system set into oscillation in a particular normal mode remains in that mode forever, and none of the others ever get excited.

Concerning the left-hand sides, one can wonder why the frequency/energy appears linearly in Eq. 11 in the quantum problem, whereas it was quadratic in the coupled oscillator calculation Eq. 4. The answer, of course, lies in the fact that Newton's equations involve $\frac{d^2}{dt^2}$, whereas the Schroedinger equation involves only $\frac{\partial}{\partial t}$.

We have exploited the translation invariances of the oscillator system and the Hubbard Hamiltonian to guess (make an *ansatz*) to extract the normal modes/band structure. In the absence of such symmetries the problem bcomes one of diagonalizing a matrix.

Put another way, we can write the Hubbard Hamiltonian as

$$\hat{\mathcal{H}} = \begin{pmatrix} \hat{c}_1^\dagger & \hat{c}_2^\dagger & \hat{c}_3^\dagger & \hat{c}_4^\dagger & \hat{c}_5^\dagger & \cdots \end{pmatrix} \begin{pmatrix} -\mu & -t & 0 & 0 & 0 & \cdots \\ -t & -\mu & -t & 0 & 0 & \cdots \\ 0 & -t & -\mu & -t & 0 & \cdots \\ 0 & 0 & -t & -\mu & -t & \cdots \\ 0 & 0 & 0 & -t & -\mu & \cdots \\ \vdots & \vdots & \vdots & \vdots & \vdots & \ddots \end{pmatrix} \begin{pmatrix} \hat{c}_1 \\ \hat{c}_2 \\ \hat{c}_3 \\ \hat{c}_4 \\ \hat{c}_5 \\ \vdots \end{pmatrix} \tag{12}$$

We happen to know (if we have some experience with tri-diagonal matrices) the eigenvalues and eigenvectors of the matrix in Eq. 12. The eigenvalues are just the $E(k)$ in Eq. 11, and the matrix of eigenvectors has entries $\Psi_{kl} = e^{ikl}$. I have used the notation Ψ deliberately, because these eigenvectors are quite literally the familiar plane-wave solutions of the free particle Schroedinger equation (on a discrete lattice). This justifies our referring to k as the momentum.

If we had not known this similarity transformation, we would have proceeded by diagonalizing the matrix by calling an appropriate BLAS/LAPACK routine. While we should (and have) avoid solving the eigenproblem numerically, it is worth emphasizing it is not at all a big deal. We shall see the utility of this way of thinking in terms of matrix diagonalization when we discuss localized modes in the non-interacting Hubbard model.

Equation 11 gives the energy of a single electron, that is the energy of the state $|k\rangle = c_k^\dagger|\mathrm{vac}\rangle$. It remains to discuss the computation of the energy with M electrons. The prescription is simple: if several electrons are present, the state $|\, k_1\, k_2\, \cdots k_M\, \rangle = c_{k_1}^\dagger c_{k_2}^\dagger \cdots c_{k_M}^\dagger |\mathrm{vac}\rangle$ has energy $E(k_1) + E(k_2) + \cdots E(k_M)$. Of course the Pauli principle forbids any of the k_i from being the same.

If we are interested in the ground state of M electrons, we fill up (occupy) the states of lowest energy. The 'Fermi Energy' is the highest energy that is occupied for M particles. The seemingly mysterious choice of the minus sign in front of the hopping parameter t makes momentum $k = 0$ have the lowest energy, with a Fermi surface enclosing it.

Once we have the dispersion relation in hand, a very important quantity is the density of states $A(\omega)$. In words, $A(\omega)d\omega$ gives the number of $E(k)$ values which like between ω and $\omega + d\omega$. Formally,

$$A(\omega) \equiv \frac{1}{N} \sum_k \delta\big(\, \omega - E(k) \,\big) \tag{13}$$

We can easily get $A(\omega)$ in the limit $N \to \infty$ where the k values become continuous

$$A(\omega) = \frac{1}{2\pi} \int_{-\pi}^{+\pi} \delta\big(\, \omega + 2t\cos(k) \,\big) = \frac{1}{\omega^2 - 4t^2} \tag{14}$$

We have used the presciption $\frac{1}{N}\sum_k \to \frac{1}{2\pi}\int dk$ in going from a sum over discrete values separated by $\frac{2\pi}{N}$ to an integral.

On a 2D square lattice, the noninteracting Hubbard Hamiltonian is

$$\hat{\mathcal{H}} = -t \sum_{l_x,l_y} \left(\hat{c}^\dagger_{l_x,l_y} \hat{c}_{l_x+1,l_y} + \hat{c}^\dagger_{l_x+1,l_y} \hat{c}_{l_x,l_y} + \hat{c}^\dagger_{l_x,l_y} \hat{c}_{l_x,l_y-1} + \hat{c}^\dagger_{l_x,l_y-1} \hat{c}_{lx,l_y} \right) - \mu \sum_{l_x l_y} \hat{c}^\dagger_{l_x,l_y} \hat{c}_{l_x,l_y} \tag{15}$$

Although it is useful to work through the algebra for practice, the result is pretty reasonable, and we will just quote it. The process is just to redo the steps of Sec. 2.1 with $l \to l_x, l_y$. The result is

$$\hat{\mathcal{H}} = \sum_{k_x,k_y} \left(E(k_x,k_y) - \mu \right) \hat{c}^\dagger_{k_x,k_y} \hat{c}_{k_x,k_y} \tag{16}$$

where

$$E(k_x,k_y) = -2t\cos(k_x) - 2t\cos(k_y) \tag{17}$$

gives the energy of an electron of momentum k_x, k_y. The energy levels of the Hubbard model on a square lattice range from $-4t \le E(k_x,k_y) \le +4t$. The bandwidth $W = 8t$.

For many fermions, we again get the energy by just summing up the single particle levels out to a maximum Fermi Energy. However, in $d > 1$ one can ask for the shape of the contour of the boundary between the occupied and unoccupied k_x, k_y. This is referred to as the 'Fermi surface' (FS). For small k_x, k_y we can expand the cosines in Eq. 17 and

$$E(k_x,k_y) \sim -4t + t\left(k_x^2 + k_y^2 \right) \tag{18}$$

and the FS is a circle about $(k_x,k_y) = (0,0)$. Thinking in analogy with $E(k) = \hbar^2(k_x^2+k_y^2)/2m$ we see that the effective mass of the fermions $m \sim 1/t$.

In general $E(k)$ is not quadratic and the FS does not have a circular topology (sphere in three dimensions). Indeed, the FS's for different fillings (number of fermions) are shown in the left panel of Fig. 3. An interesting feature of the dispersion relation of Eq. 17 is 'perfect nesting'. As seen in the right panel of Fig. 3, when the interior of the FS encompasses half of the allowed momenta $-\pi < k_x, k_y < +\pi$ (and hence the lattice is half-filled), the FS is a 'rotated square' and has the feature that a single wave-vector $(k_x,k_y) = (\pi,\pi)$ connects many points on the FS. This phenomenon is referred to as 'nesting'.

The second is a 'van Hove singularity' in the density of states.

It turns out that both of these properties make the square lattice Hubbard model particularly prone to assuming ordered phases when the interaction U is turned on. The rough reason appeals to your knowledge of second order perturbation theory, where you know the effect of a perturbation $\hat{V}$ is to shift the energy E_n of eigenstate $|n\rangle$ by $E^{(2)}{}_n = \sum_{m\neq n} \frac{|\langle n|\hat{V}|m\rangle|^2}{E_n - E_m}$. If there are many states with $E_m = E_n$ the effect of $\hat{V}$ will be very large and this is precisely what happens with perfect nesting.
are materials like the cuprate superconductors for which the square lattice is appropriate.

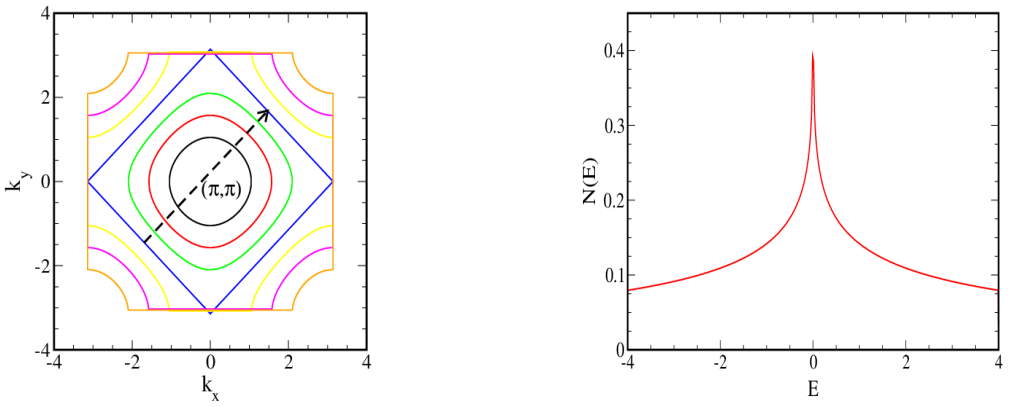

Fig. 1: *Left: The Fermi surfaces of the Hubbard model an a square lattice with nearest neighbor hopping. Right: The density of states of the Hubbard model an a square lattice with nearest neighbor hopping. There is a divergence ('van Hove singularity') of $N(\omega)$ at $\omega = 0$ (half filling).*

An interesting feature of the square lattice is that its sites can be divided into two sublattices (red and green in the left panel of Fig. 2) such the near neighbors of red sites are always green and the near neighbors of green sites are always red. Such a geometry is said to be 'bipartite', and this property has deep implications for the physics.

The honeycomb lattice describing the positions of the carbon atoms in a sheet of graphene is also bipartite. In both the square and honeycomb cases, the numbers of red and green sites are identical. We will next consider the Hubbard model on a Lieb lattice, shown in Fig. **??**.

Although we blitzed through going from a 1D chain to a 2D square lattice, it is worth being a bit more careful with this one, because going to momentum space does not quite complete the process of diagonalization.

Aside: The serious student of the Hubbard model would do well to compute $E(k_x, k_y)$ for a honeycomb geometry. This is useful 'technical' practice, as dealing with axes which are not parallel to $\hat{x}$ and $\hat{y}$ requires some care. It is also of course very interesting physically towards the understanding of graphene. Just as the dispersion relation of the square lattice has interesting properties like Fermi nesting,.

Examining Eqs. 5 and 5, it is clear that disorder in the hoppings or chemical potentials (making the energy for a fermion to occupy a particular location site-dependent) can be simply incorporated by changing the matrix elements. The transformation Eq. 6 no longer diagonalizes the Hamiltonian, as translation invariance is broken. However the diagonalization can still be accomplished numerically.

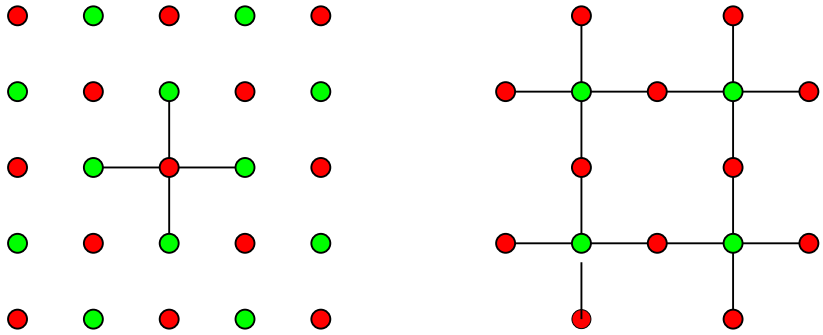

Fig. 2:

A very interesting phenomenon occurs. While the plane wave eigenstates in the absence of randomness extend throughout the lattice, the eigenstates in the presence of disorder can be 'localized', meaning that the components of the eigenstate are significant only on a fraction of the sites and exponentially small elsewhere. In the generic situation the eigenstates near the center of the DOS are delocalized, and those the edges (high and low energies) are localized, with a 'mobility edge' separating the two cases.

Here one can return to the analogy with classical systems, and a beautiful discussion of Maradudin which describes localization about a single defect mass in a 1D mass-spring chain **??**.

There is a lot to unpack in the comments above, and indeed there was an effort over more than a decade to understand the nature of localization in two dimensions. But the main message for us here is that many aspects of this deep and beautiful chapter of condensed matter physics conform to the title of this chapter: From a computational perspective they boil down to the very familiar and simple question of diagonalizing a matrix!
A recently emerging area of interest concerns non-Hermitian Hamiltonians. The simple methods we have introduced give us a foothold into this field as well.
??

For concreteness, let's consider the 'Hatano-Nelson Hamiltonian' in one dimension:

$$\hat{\mathcal{H}} = -t \sum_{l=1}^{L} (e^{h}\, \hat{c}_{l+1}^{\dagger} \hat{c}_{l} + e^{-h}\, \hat{c}_{l}^{\dagger} \hat{c}_{l+1}) + \sum_{l} \mu_{l}\, \hat{c}_{l}^{\dagger} \hat{c}_{l} \quad . \tag{19}$$

which is obtained from the Hubbard model of Eq. **??** by introducing a hopping which is different for fermions moving to the left and to the right. The parameter h controls the degree of anisotropy in the hopping, and μ_l are random site energies. Periodic boundary conditions connect sites 1 and L.

In the case where there is no disorder, $\mu_l = 0$, we can try the same canonical transformation as Eq. 6, which leads to eigenvalues then have the form,

$$E(k) = t(e^{-h-ik} + e^{h+ik}) \ . \tag{20}$$

As k varies from 0 to 2π (in steps of $\frac{1}{L}$) this describes an ellipse centered at the origin of the complex plane. The length of the ellipse along the real axis is $4t\cosh h$ and along the imaginary axis, $2t\sinh h$. The periodic boundary conditions are crucial. Without them one can do a 'gauge transformation', or in more elementary language a redefinition of the eigenvectors, which makes h disappear from the problem: $\tilde{v}_l = e^{-hl} v_l$. Then the matrix is Hermitian, with all real eigenvalues.

As remarked earlier, in the presence of disorder the transformation of Eq. 6 no longer works. Instead one simply diagonalizes the matrix,

$$H = \begin{pmatrix} \mu_1 & -\frac{t}{2}e^{h} & 0 & 0 & 0 & \cdots & -\frac{t}{2}e^{-h} \\ -\frac{t}{2}e^{-h} & \mu_2 & -\frac{t}{2}e^{h} & 0 & 0 & \cdots & 0 \\ 0 & -\frac{t}{2}e^{-h} & \mu_3 & -\frac{t}{2}e^{h} & 0 & \cdots & 0 \\ \vdots & \vdots & \vdots & & & \vdots & \ddots \\ -\frac{t}{2}e^{h} & 0 & 0 & 0 & 0 & -\frac{t}{2}e^{-h} & \mu_L \end{pmatrix} \tag{21}$$

With periodic boundary conditions, the eigenvalue distribution consists of an ellipse centered at the origin of the complex plane, with wings extending out from the ellipse along the real axis. The eigenvectors associated with the real eigenvalues on the wings are localized, and those on the wings are real. The plausibility argument for this assertion is that even with periodic boundary conditions one can in fact accumulate the h factors on any desired link (or set of links) through suitable gauge transformations. For a localized eigenvector one can move all the h factors to a lattice location where the wave function is arbitrarily (exponentially) small. So those eigenvectors are governed by a piece of H which can be made Hermitian in the only part of the lattice that matters to them. They will have real eigenvalues. This doesn't work for extended eigenvectors, so they have complex eigenvalues.

New Information:

If the disordered site energies are taken from the Cauchy distribution,

$$p(\mu_l) = \frac{1}{\pi} \frac{\gamma}{\gamma^2 + \mu_l^2} \ , \tag{22}$$

then what happens is this: The height of the ellipse (parallel to the imaginary axis), gets reduced by γ while the base of the ellipse (parallel to the real axis) remains fixed! Since the ellipse height in the imaginary direction is $\sinh h$ (with $t = 1$), the ellipse gets completely squashed down when γ exceeds a critical value $\gamma_c = \sinh h$. The eigenspectrum is completely real for $\gamma > \gamma_c$.

We can of course equivalently think about it from the viewpoint of Carl's question of a critical degree of non-Hermiticity. If the disorder γ is fixed, the eigenspectrum remains real until h exceeds a threshold value $h_c = \sinh^{-1}\gamma$.

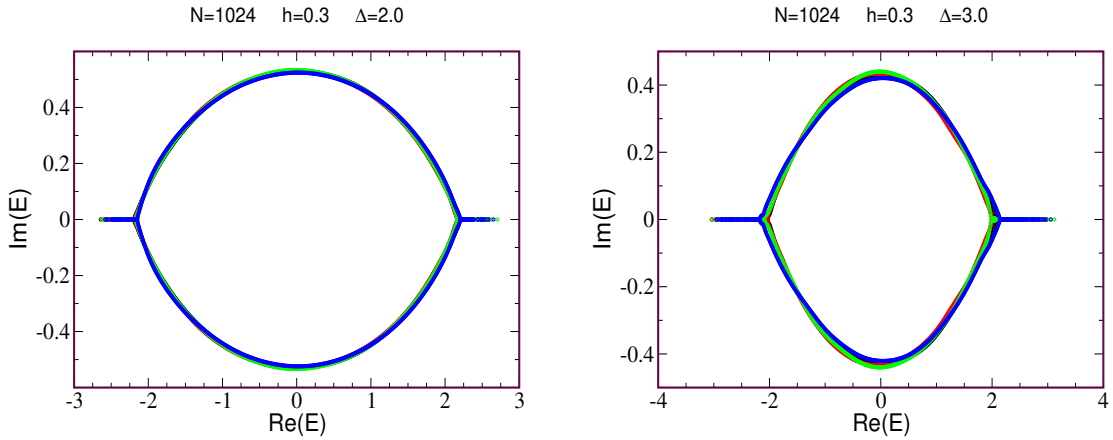

Fig. 3: *Left: The Fermi surfaces of the Hubbard model an a square lattice with nearest neighbor hopping. Right: The density of states of the Hubbard model an a square lattice with nearest neighbor hopping. There is a divergence ('van Hove singularity') of $N(\omega)$ at $\omega = 0$ (half filling).*

I am not quite sure about this, but I infer from the Figures in Zickel's thesis, that the total range of the eigenvalues in the real direction, from tip of wing to tip of wing, depends only on γ and not on h. Thus it looks to me as if eventually the real wings will go away when the ellipse axis in the real direction, cosh$h$, exceeds the real extent of the total eigenspectrum, which is fixed by γ. Again, I need to double check this. If true, then as h is increased from $h = 0$ one would have two transitions, from all real spectrum to mixed (part real, part complex) at $h_{c1} = \sinh^{-1}\gamma$, and then from mixed to all complex at h_{c2}.

3 Mean Field Theory

4 Particle-Hole Symmetry

5 Staggered Particle-Particle Transformation

```
\vskip0.07in
Review usual stuff all from viewpoint of U>0:
t=0 limit
U=0 limit
   Emphasis on cool physics form matrix diagonalization!
   Here describe the flat band models of Kagome, Lieb.
   Mention BEC in flat bands (our paper)?
   Nesting?  DOS?
Mott transition
J=t^2/U (lead in to AF discussion)
```

```
\vskip0.07in
But then focus on canonical transformations  (access U<0)
   +U to -U
   eta pairing from Nagaoka
   Huaming work
```

Appendices

A Some remarks

The appendix part should be deleted if no appendices are necessary.

References

[1] Patrik Fazekas: *Lecture Notes on Electron Correlation and Magnetism* (World Scientific, Singapore, 1999)

[2] T. Esslinger, Annu. Rev. Condens. Matter Phys. 1, 129 (2010).

[3] L. Tarruell and L. Sanchez-Palencia, Comptes Rendus Physique 19, 365 (2018).

[4] J. Zaanen and O. Gunnarsson, Physical Review B 40, 7391, (1989).

[5] J.P.F. LeBlanc *etal*, Phys. Rev. X 5, 041041 (2015).

[6] S.R. White and D.J. Scalapino, Physical Review Letters 91, 136403, (2003).

[7] K. ChŃg, J. Carrasquilla, R.G. Melko, and E. Khatami, Physical Review X 7, 031038, (2017).

[8] D.P. Arovas, E. Berg, S.A. Kivelson, and S. Raghu, Annual review of condensed matter physics 13, 239 (2022).

[9] A.A. Maradudin, P. Mazur, E.W. Montroll, and G.H. Weiss, Reviews of Modern Physics 30, 175, (1958).

[10] J. Feinberg and A. Zee, Nucl. Phys. **B504**, 579 (1997);